Intramolecular Vibrational Dynamics in Free Polyatomic Molecules with C=O Chromophore Bond Excited by Resonant Femtosecond IR Laser Radiation

ARTICLE *in* THE JOURNAL OF PHYSICAL CHEMISTRY A · JANUARY 2014

Impact Factor: 2.69 · DOI: 10.1021/jp407131x · Source: PubMed

7 AUTHORS, INCLUDING:

S.V. Chekalin
Institute of Spectroscopy of the USSR Acade…
231 PUBLICATIONS **1,167** CITATIONS
SEE PROFILE

Victor Kompanets
Institute of Spectroscopy of the USSR Acade…
94 PUBLICATIONS **319** CITATIONS
SEE PROFILE

Pavel Koshlyakov
Russian Academy of Sciences
17 PUBLICATIONS **32** CITATIONS
SEE PROFILE

V. B. Laptev
Russian Academy of Sciences
49 PUBLICATIONS **162** CITATIONS
SEE PROFILE

THE JOURNAL OF PHYSICAL CHEMISTRY A

Article

pubs.acs.org/JPCA

Intramolecular Vibrational Dynamics in Free Polyatomic Molecules with C═O Chromophore Bond Excited by Resonant Femtosecond IR Laser Radiation

Sergey V. Chekalin,[†] Victor O. Kompanets,[†] Pavel V. Koshlyakov,[‡] Vladimir B. Laptev,*[,†] Sergey V. Pigulsky,[†] Alexander A. Makarov,[†] and Evgeny A. Ryabov*[,†]

[†]Institute of Spectroscopy, Russian Academy of Sciences, Fizicheskaya street, 5, Troitsk, Moscow 142190, Russia

[‡]Voevodsky Institute of Chemical Kinetics and Combustion, Siberian Branch of the Russian Academy of Sciences, Institutskaya street, 3, Novosibirsk 630090, Russia

ABSTRACT: In nine polyatomic molecules, we have studied the intramolecular redistribution of vibrational energy from chromophore C═O group excited by a resonant femtosecond IR laser radiation at a wavelength of ∼5 μm. All experiments have been performed in the gas phase using the IR−IR pump−probe technique in combination with the spectral analysis of the probe radiation. For molecules with one C═O end group, characteristic times of intramolecular vibrational redistribution (IVR) lie in the range between 2.4 and 20 ps and correlate with the density of four-frequency Fermi resonances. The IVR times in metal carbonyl molecules are anomalously long, being ∼1.0 ns for $Fe(CO)_5$ and ∼1.5 ns for $Cr(CO)_6$. In the $CH_3(C{=}O)OC_2H_5$ and $H_2CCH(C{=}O)OC_2H_5$ molecules, it has been observed that there are two characteristic IVR times, which differ by an order of magnitude from each other; this was interpreted in terms of the developed model of "accumulating states". For the ICF_2COF molecule, it has been revealed that the IVR time decreases with increasing level of the vibrational excitation of the C═O bond of the molecule.

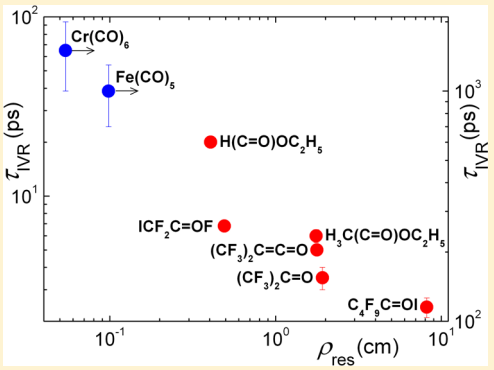

I. INTRODUCTION

Multiphoton excitation of a polyatomic molecule in the ground electronic state that is selective with respect to a singled out vibrational mode is restricted[1−3] by the process of the energy redistribution from the pumped mode to other vibrations of the molecule (intramolecular vibrational redistribution (IVR); see refs 4−8 for a review). Creation of sources of coherent femtosecond radiation in the mid-IR range enables realization of photochemical transformations in molecules that are selective with respect to a bond or a group of bonds and that occur prior to the vibrational energy will become statistically redistributed over remaining modes. In refs 9 and 10, it has been reported that, upon resonant multiphoton excitation of vibrations of C═N═N and C═O bonds in diazomethane and metal carbonyls in the gas phase by femtosecond IR laser pulses, the character of dissociation of molecules of these compounds is nonstatistical. By virtue of specific features of their chemical bond, these molecules have rather low activation energies, 35−40 kcal/mol (12 000−14 000 cm^{-1}). Attempts to realize photochemical reactions in ordinary molecules with covalent bonds and activation energies higher than 50 kcal/mol (>17 500 cm^{-1}) using femtosecond IR radiation have yet failed.[11] Therefore, there is a need to study in more detail the dynamics of intramolecular processes that proceed after the IR multiphoton excitation of a chosen vibrational mode.

In experiments on the IR multiphoton excitation of $W(CO)_6$ molecules dissolved in *n*-hexane, it has been observed that, 1 ps after the pulse pump, the T_{1u} resonant mode of vibrations of C═O bonds was populated up to a vibrational level with $v = 6$ (∼12 000 cm^{-1}).[12] However, it is rather problematic to study the intramolecular dynamics under these conditions because it is difficult to take into account the influence of the solvent.[13,14]

Previously, investigations of the IVR in *free* molecules in the gas phase have been performed with molecules of propyne $HC{\equiv}CCH_3$ and its derivatives in the picosecond range. In these experiments, an IR pulse of the pump radiation produced a one-quantum excitation of vibrations of the H−C≡ bond (∼3330 cm^{-1}). To probe excited vibrational states, the methods of IR absorption[15−17] and time-resolved Raman scattering[18−23] were used. Characteristic IVR times, τ_{IVR}, measured in these experiments lie in the range from tens of picoseconds to a few nanoseconds. An analysis of results obtained in ref 15 made it possible to separate the IVR process from the process of vibrational energy transfer to solvent molecules. However, to do this separation, it was necessary to conduct parallel experiments in the solvent and in the gas phase.

Received: July 18, 2013
Revised: January 24, 2014

   dx.doi.org/10.1021/jp407131x | J. Phys. Chem. A XXXX, XXX, XXX−XXX

The vibrational dynamics induced in *free* $W(CO)_6$ molecules (the gas phase) as a result of the *one-photon* excitation of the vibration of the C═O bond has been studied in ref 24 using the IR−IR pump−probe method with a time resolution of ~40 ps. For this molecule, a rather slow intramolecular relaxation of the vibrational energy from the excited mode with a characteristic time of $\tau_{IVR} \approx 1.3$ ns was observed. One can assume that so slow rate of the IVR from vibrational modes of the C═O bond is characteristic for all metal carbonyl molecules of this type. It seems that precisely this circumstance explains the mode-selective character of the excitation of $Fe(CO)_5$ molecules, which, as was stated in ref 9, took place up to the dissociation limit.

The next step has been made in our studies[25,26] of the vibrational dynamics in different modes of the $(CF_3)_2C═C═O$ molecule, in which the mode $\nu_1 = 2194$ cm^{-1} of the asymmetric vibration of the C═C═O bond was excited by resonant femtosecond IR radiation. It was shown that the selective multiphoton excitation of this mode takes place, which is noticeable up to the level $v = 7$. The subsequent relaxation of the excitation from the ν_1 mode in the course of the IVR occurred with a characteristic time of $\tau_{IVR} \approx 5$ ps. We revealed the appearance of an instantaneous ($\tau \ll \tau_{IVR}$) signal of an induced absorption in the nonresonant modes $\nu_2 = 1417$ cm^{-1} (symmetric vibration of the C═C═O bond), $\nu_3 = 1340$ cm^{-1}, and $\nu_4 = 1194$ cm^{-1} (different collective vibrations of CF bonds). The form of the subsequent evolution of this signal and its corresponding characteristic times proved to be different for different modes, which, in our opinion, was related to the occurrence of different pathways for the vibrational energy migration in the molecule.

In this work, we present results of our further investigations into the vibrational dynamics in a series of molecules with the C═O chromophore group, which was excited by resonant femtosecond IR radiation.

II. EXPERIMENTAL SETUP

To study the vibrational dynamics, we used the IR−IR pump−probe method. As IR radiation sources, we used two nonlinear converters based on TOPAS-C optical parametric amplifiers (OPAs) with subsequent difference frequency generation in a DFG-1 unit (Light Conversion). The radiation frequencies of the converters can be tuned independently from each other. One of these converters was used as a pump source, while the other one, as a probe source. These OPAs were synchronously pumped with a femtosecond Ti:Sapphire laser (Spectra-Physics) ($\lambda = 800$ nm; pulse duration and energy, 50 fs and 1.2 mJ, respectively). The radiation from the second OPA was split by a CaF_2 wedge into two beams and was used to form probe and reference beams. The pump and probe beams were focused by CaF_2 lenses and were reunited at an angle of about 9° such that the waist of the probe beam was embedded in the waist of the pump beam. The transverse and longitudinal energy distributions of the pump and probe beams were measured with a Pyrocam III pyroelectric array. The polarizations of the pump and probe pulses were perpendicular to each other. The cell (4.8 mm long, CaF_2 windows) with a gas under study was placed in the intersection region of the waists. The reference beam passed through the cell at a certain distance from the intersection of the waists. After the cell, the probe and reference beams were focused onto the entrance slit of a monochromator. The radiation intensities I_{probe} and I_{ref} of the beams emergent from the monochromator were measured with two HgCdTe cooled detectors. The magnitude of the induced absorption was defined as

$$\Delta k_{OD} = \log_{10}\left(\frac{(I_{probe}/I_{ref})_{pump}}{(I_{probe}/I_{ref})_{gas}}\right) \quad (1)$$

where the subscripts "pump" and "gas" refer to the values of the ratio I_{probe}/I_{ref} in the presence and in the absence of the pump, respectively. According to formula 1, a positive value of $\Delta k_{OD}(\tau_d)$ corresponds to a bleaching of the absorption. The amplitude and the spectrum of the signal Δk_{OD} were measured versus the delay τ_d between the pump and probe pulses. The repetition rate of femtosecond pulses was 1 kHz, the energy of the pump pulse at a wavelength of 5 μm was up to 14 μJ, the pulse duration at half-height inside the cell was 150 fs, and the spectral width of the radiation was 240 cm^{-1}. In the majority of measurements, the spectral bandpass of the monochromator was 3−5 cm^{-1}. The flux density of the pump energy (energy fluence) inside the cell did not exceed $\Phi_{pump} \approx 80$ mJ/cm^2. The vapor pressure of compounds under study was chosen such that not more than half of the pump energy would be absorbed along the cell length and was varied from 0.1 Torr (13.3 Pa) for $Cr(CO)_6$ to 100 Torr (13.3 kPa) for $(CF_3)_2C═O$. At these pressures, perturbations related to the intermolecular interaction can be ruled out almost completely.

As objects of study, we used molecules of compounds of different classes, such as $Fe(CO)_5$, $Cr(CO)_6$, $(CF_3)_2C═C═O$, $(CF_3)_2C═O$, $C_4F_9C═OI$, $ICF_2C═OF$, $H(C═O)OC_2H_5$, $CH_3(C═O)OC_2H_5$, and $H_2C═CH(C═O)OC_2H_5$, all having the C═O molecular chromophore group, which can be excited by femtosecond radiation with a wavelength in the range of 5 μm. The content of the base substance in the used gas samples was not lower than 99%, which was controlled by IR spectroscopy, or was specified by the manufacturer.

The technique that we use is based on the measurement of the IR absorption induced in the mode to be probed. As is known, the transition cross-section between levels of a harmonic oscillator increases linearly with the level number, which also holds with a good accuracy for an anharmonic oscillator. Since, in this case, the magnitude of the absorption is determined by the *difference* between the populations for corresponding transitions, then it can be easily verified that the magnitude of the absorption integrated over all levels (and, correspondingly, over the spectrum) does not depend on the energy stored in the probed mode. At the same time, the anharmonicity of vibrations leads to a situation that, as the molecule becomes excited, the position (and the shape) of the vibrational spectrum can noticeably change, shifting, as a rule, toward the red range. Precisely these changes of the spectrum, which were taken in a narrow spectral interval that was selected by the monochromator, were measured and considered in this work.

III. EXPERIMENTAL RESULTS

All investigated molecules have a strong and fairly isolated vibration of the C═O bond, to resonance with which the femtosecond pump radiation was tuned. In experiments, we studied the excitation and subsequent IVR from the resonant mode. The spectra of the pump and probe pulses in these measurements coincided with each other. A narrow spectral interval that the monochromator selected from the spectrum of the probe beam was successively shifted from the center of the absorption band of the C═O bond toward the long-

dx.doi.org/10.1021/jp407131x | J. Phys. Chem. A XXXX, XXX, XXX−XXX

wavelength range by a value that was multiple of the expected anharmonicity value, which, for the vibration of the C=O bond, usually is 20−25 cm^{-1}. This allowed us to measure kinetic dependences for successive vibrational transitions of the resonant mode.

Examples of typical kinetic dependences $\Delta k_{OD}(\tau_d)$ that were obtained for $ICF_2C{=}OF$, $H(C{=}O)OC_2H_5$, and $C_4F_9C{=}OI$ molecules at probe frequencies corresponding to the vibrational transition $v = 0 \rightarrow v = 1$ of the excited mode are presented in Figure 1. For each of these curves, an exponential decay of the signal is observed, with the characteristic time of which being individual for a particular molecule. The characteristic times for all molecules under study are presented in Table 1.

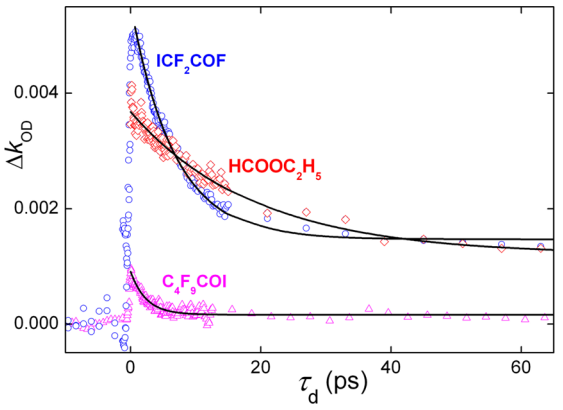

Figure 1. Dependences of the signal Δk_{OD} for the vibrational transition 0−1 on the delay time τ_d for molecules $ICF_2C{=}OF$, $H(C{=}O)OC_2H_5$, and $C_4F_9C{=}OI$. Solid curves are approximations by a single exponential.

A characteristic feature of the dependences in Figure 1 is that, after the initial exponential decay, the observed kinetic curves attain a certain constant level, which, for different molecules, amounts to 10−45% of the maximal signal. We believe that the magnitude of this constant level is determined by the excess energy in all the modes of the molecule, which is acquired as a result of the redistribution of the absorbed energy. Indeed, intermode anharmonic shifts as a result of an energy increase in modes of the molecule (especially, low-frequency ones) lead to a statistical inhomogeneous broadening of the band (see ref 27) and to its shift as a whole, compared to the shape of the band before the excitation. This broadening gives rise to a stationary signal from heated molecules at the used probe frequencies, including those of lowest transitions.

Similar kinetic dependences, including those for higher-lying vibrational transitions, were also obtained for other molecules. For the majority of dependences, the decay curves were approximated by a function $A_0 + B \exp(-\tau_d/\tau_{IVR})$, where A_0 and B are approximation constants, τ_d is the time of delay between pulses, which was varied in experiments. For two molecules, ethyl acetate $H_3C(C{=}O)OC_2H_5$ and ethyl acrylate $H_2C{=}CH(C{=}O)OC_2H_5$, we used a biexponential approximation $A_0 + B_1 \exp(-\tau_d/\tau_1) + B_2 \exp(-\tau_d/\tau_2)$. The characteristic times obtained in this way are presented in Table 1.

Certain additional measurements will be discussed in the next section.

IV. DISCUSSION

With respect to the location of the chromophore C=O group in the molecule, all the investigated compounds can be divided into three types. Molecules with only one C=O chromophore, such as $(CF_3)_2C{=}C{=}O$, $(CF_3)_2C{=}O$, $C_4F_9C{=}OI$, $ICF_2C{=}OF$, and $H(C{=}O)OC_2H_5$, are grouped into the first class. In molecules of the second type, the C=O chromophore is located in the middle (inside) of the molecule ($H_3C(C{=}O)OC_2H_5$ and $H_2CCH(C{=}O)OC_2H_5$). Finally, molecules of the third type have several C=O groups each, and these groups surround the central atom ($Fe(CO)_5$ and $Cr(CO)_6$). We note that the molecules of the latter group noticeably differ from the molecules of the former two groups by a higher symmetry (D_{3h} and T_{1u}) and by the donor−acceptor type of the C=O group bonding with the central atom. It can be seen from Table 1 that the intramolecular dynamics in molecules of different types is different.

Molecules of the first type distinguish themselves by a simple character of the IVR and by a relatively short times τ_{IVR}, which are in the range between 2.4 and 20 ps. Contrary to the compounds of the first type, for molecules of iron and chromium carbonyls, the values of τ_{IVR} lie in the nanosecond range, i.e., differ from the IVR times of the remaining molecules almost by two to three orders of magnitude. By virtue of certain experimental restrictions, the kinetic dependences for these molecules were obtained on a relatively short time interval, 200 ps. Therefore, we only estimated the values of their characteristic time τ_{IVR} of the IVR process, which proved to be 1.0 ± 0.3 ns for $Fe(CO)_5$ and 1.5 ± 0.5 ns for $Cr(CO)_6$.

Table 1. Characteristic Times τ_{IVR} of Intramolecular Relaxation at the Vibrational Transition 0−1 for Investigated Molecules upon Excitation of the Vibration of the C=O Bond

	molecule	frequency of the excited vibration ν_{CO}, cm^{-1}	τ_{IVR}, ps	average vibrational energy $\langle E_{vib}\rangle$ at T = 293 K, cm^{-1}	notes
type 1	$C_4F_9C{=}OI$	1793	2.4 ± 0.3	2668	
	$(CF_3)_2C{=}O$	1804	3.5 ± 0.5	1255	
	$(CF_3)_2C{=}C{=}O$	2194	5.0 ± 0.3	1501	vibration of the C=C=O bond
	$ICF_2C{=}OF$	1880	6.8 ± 0.2	853	
	$H(C{=}O)OC_2H_5$	1750	20 ± 1	593	
type 2	$H_3C(C{=}O)OC_2H_5$	1756	τ_1 = 6 ± 1 τ_2 = 75 ± 20	1121	biexponential decay $B_1 \approx (2.8{-}3.3)B_2$
	$H_2CCH(C{=}O)OC_2H_5$	1751	τ_1 = 8 ± 1.5 τ_2 = 80 ± 20		biexponential decay $B_1 \approx (0.7{-}0.9)B_2$
type 3	$Fe(CO)_5$	2014	(1.0 ± 0.3) × 10^3	2414	estimate
	$Cr(CO)_6$	2000	(1.5 ± 0.5) × 10^3	1883	estimate

dx.doi.org/10.1021/jp407131x | J. Phys. Chem. A XXXX, XXX, XXX−XXX

They agree with the value $\tau_{IVR} \approx 1.3$ ns that was measured in ref 24 for a similar $W(CO)_6$ molecule. The kinetic dependences of the signal $\Delta k_{OD}(\tau_d)$ for the second-type molecules with the internal C═O chromophore group (ethyl acetate $H_3C(C{=}O)OC_2H_5$ and ethyl acrylate $H_2CCH(C{=}O)OC_2H_5$) have a clearly pronounced specific feature, compared to the other molecules, because they are biexponential with two strongly different characteristic times (see Figure 2). Almost all kinetics obtained for these molecules at different frequencies within the limits of the absorption band of the C═O bond have the same biexponential character.

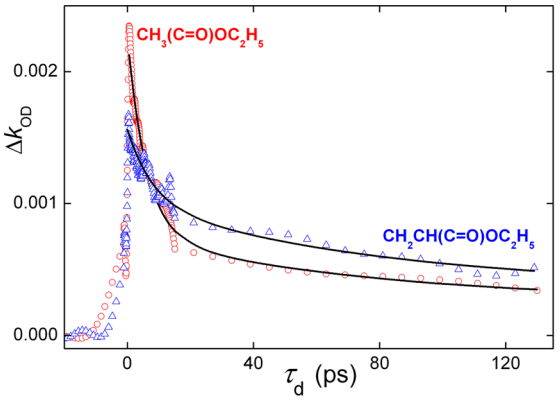

Figure 2. Dependences of the signal Δk_{OD} for the vibrational transition 0−1 on the delay time τ_d for molecules $H_3C(C{=}O)OC_2H_5$ and $H_2CCH(C{=}O)OC_2H_5$. Solid curves are approximations.

In further sections, we will discuss to what extent experimentally measured IVR times correlate with certain spectroscopic characteristics of investigated molecules.

A. Density of States. It was often supposed that, for the vibrational energy to be stochastic (random), it is necessary to attain states with a certain density of vibrational levels.[4] Consequently, under certain conditions, the intramolecular relaxation time can correlate with the density of vibrational states ρ_{vib} in the vicinity of the excited level. For each molecule, we calculated the values of ρ_{vib} for the energy that is equal to the sum of the quantum of the mode ν_{CO} and the average equilibrium vibrational energy $\langle E_{vib}\rangle$ of the molecule. Since the spectrum of the excitation radiation covered completely the IR absorption band of the molecule, and the entire initial vibrational−rotational distribution interacted with the radiation, the value of $\langle E_{vib}\rangle$ was estimated for the Boltzmann distribution at room temperature (T = 293 K). The frequencies of vibrations for molecules $Fe(CO)_5$, $Cr(CO)_6$, $(CF_3)_2C{=}C{=}O$, $(CF_3)_2C{=}O$, and $H(C{=}O)OC_2H_5$ that are necessary for the calculation of the values of $\langle E_{vib}\rangle$ and $\rho_{vib}(\langle E_{vib}\rangle + h\nu_{CO})$ were taken from the literature, and for the remaining molecules, they were partially taken from IR spectra that we measured and partially determined from quantum-mechanical calculations. Calculations were done using the Gaussian 98 software package by the DFT−B3LYP method with the basis sets aug-cc-pVTZ for $H_3C(C{=}O)OC_2H_5$ and DEF2-TZVPPD for $C_4F_9C{=}OI$ and $ICF_2C{=}OF$.

In Figure 3, results of calculations of ρ_{vib} along with experimentally measured values of τ_{IVR} are plotted in corresponding coordinates. For all the molecules that we examined, except for $H(C{=}O)OC_2H_5$, the density of states at a given energy is greater than or on the order of 10^3 cm, which is usually considered to be more than sufficient for the IVR

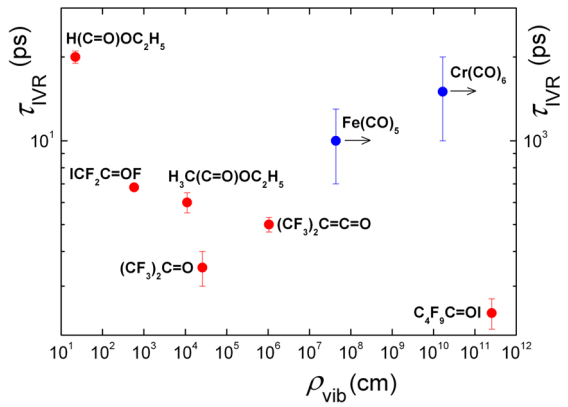

Figure 3. Relationship of the characteristic IVR times τ_{IVR} for different molecules with the density of vibrational states ρ_{vib} at the level $\langle E_{vib}\rangle + h\nu_{CO}$ (see text).

effect to take place (see, e.g., refs 15, 28, and 29). A monotonic tendency can be seen for the group of molecules with a single C═O chromophore. To a greater density of states, a shorter IVR time corresponds. However, it has been repeatedly noted that the correlation of this kind is not universal. This is confirmed by a sharp dissonance between the behavior of metal carbonyls $Fe(CO)_5$ and $Cr(CO)_6$ (see the right upper part of Figure 3) and the behavior of the remaining molecules.

A far more universal correlation is that between the IVR time and the density of intermode anharmonic resonances, which was noted as early as in ref 30. An example that illustrates this situation was given in 31. On the basis of the density of resonances (more exactly, on the density of states in nearest "tiers" (for the tier model, see, e.g., refs 32 and 33 and refs in 31), which are coupled to the initial state by a chain of three- and four-frequency resonances), the authors of ref 31 explained the difference between the times of the IVR from the ν_{HC} mode in two molecules of the same type, $HC{\equiv}CC(CH_3)_3$ and $HC{\equiv}CSi(CH_3)_3$, which was experimentally measured in ref 34. In the $HC{\equiv}CSi(CH_3)_3$ molecule, which is heavier and, correspondingly, has a higher density of states, this IVR time paradoxically proved to be longer by more than an order of magnitude. Our situation is similar and, as will be seen in the next subsection, a dramatic difference between the IVR times in metal carbonyls and remaining investigated molecules can, indeed, be explained by a strong qualitative difference in the structure of intermode resonances.

B. Density of Intermode Anharmonic Resonances. To reveal the occurrence of correlations between IVR times and densities of intermode resonances, we calculated for each molecule the number of three- and four-frequency resonances with energy defects ≤20 and ≤10 cm^{-1}, respectively. The resonance condition was defined as $\nu_{CO}-\nu_i-\nu_j \leq 20$ cm^{-1} for the three-frequency resonance and as $\nu_{CO}-\nu_i-\nu_j \pm \nu_k \leq 10$ cm^{-1} for the four-frequency one. The plus sign in the expression for the four-frequency resonances corresponds to transitions in the ν_{CO} mode in hot bands, and each of these resonances was taken into account with its own statistical weight, equal to the relative population of the hot level. In order to indirectly take into account a stronger interaction between the vibration of the mode to be excited and resonant sets of vibrations in the case of three-frequency resonances compared to four-frequency ones, the energy interval for their calculation was increased 2-fold. Results of calculations are presented in Table 2 and are shown in Figure 4.

dx.doi.org/10.1021/jp407131x | J. Phys. Chem. A XXXX, XXX, XXX−XXX

Table 2. Number of Three-Frequency Resonances with Defects ≤20 cm^{-1} and Their Average Density vs τ_{IVR} for Molecules under Study

molecule	τ_{IVR}, ps	number of three-frequency Fermi resonances in ±20 cm^{-1}	density of three-frequency Fermi resonances, cm	detunings from nearest resonances that do not fall into the interval ±20 cm^{-1}, cm^{-1}
C_4F_9COI	2.4 ± 0.3	15	0.375	$\nu_9 + \nu_{17} - \nu_1 = 21$
				$\nu_3 + \nu_{23} - \nu_1 = -21$
$(CF_3)_2CO$	3.5 ± 0.5	6	0.15	$\nu_{13} + \nu_{20} - \nu_1 = 41$
				$\nu_3 + \nu_{19} - \nu_1 = -23$
$(CF_3)_2CCO$	5.0 ± 0.3	2	0.05	$\nu_{15} + \nu_{16} - \nu_1 = 79$
				$\nu_{10} + \nu_{16} - \nu_1 = -46$
ICF_2COF	6.8 ± 0.2	0	0	$\nu_2 + \nu_7 - \nu_1 = 23$
				$\nu_4 + \nu_6 - \nu_1 = -27$
$H_3C(CO)OC_2H_5$	τ_1 = 6 ± 1	9	0.225	$\nu_{13} + \nu_{30} - \nu_9 = 29$
				$\nu_{11} + \nu_{31} - \nu_9 = -46$
$H(CO)OC_2H_5$	20 ± 1	4.41	0.110	$\nu_9 + \nu_{16} - \nu_5 = 29$ trans
				$\nu_7 + \nu_{26} - \nu_5 = -21$ trans
				$\nu_6 + \nu_{25} - \nu_5 = 21$ gauche
				$\nu_7 + \nu_{17} - \nu_5 = -31$ gauche
$Fe(CO)_5$	$(1.0 \pm 0.3) \times 10^3$	0	0	$\nu_6 + \nu_{15} - \nu_{10} = 95$
$Cr(CO)_6$	$(1.5 \pm 0.5) \times 10^3$	0	0	$\nu_3 + \nu_{13} - \nu_6 = 95$

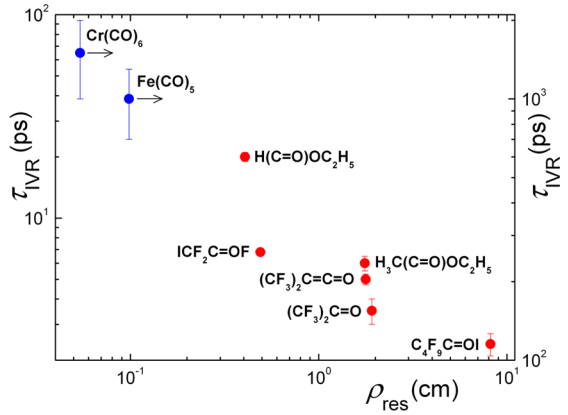

Figure 4. Dependence of characteristic intramolecular relaxation times τ_{IVR} for different molecules on the density of four-frequency resonances ρ_{res} with defects ≤10 cm^{-1}.

Even in the case of three-frequency resonances for different groups of molecules, a certain correlation between their density and IVR time is observed. Thus, in the group of halogen-substituted molecules $ICF_2C{=}OF$, $(CF_3)_2C{=}C{=}O$, $(CF_3)_2C{=}O$, and $C_4F_9C{=}OI$, an increase in the density of resonances from conventional zero to 0.375 cm corresponds to a monotonic decrease in τ_{IVR} from 6.8 to 2.4 ps. Similarly, upon replacement of the hydrogen atom in the H−C=O group of the $H(C{=}O)OC_2H_5$ molecule by the CH_3 group, a more complex $CH_3(C{=}O)OC_2H_5$ molecule is formed; in this case, the density of resonances increases from 0.110 to 0.225 cm, while the IVR time decreases from 20 to 6 ps. We also note that, for almost all molecules, except for metal carbonyls, nearest resonances that fall out of the interval ≤20 cm^{-1} are spaced at a distance from a few to ten reciprocal centimeters (see the last column of Table 2). This testifies to a quite high average density of resonances compared to metal carbonyls; therefore, it seems that the absence of three-frequency resonances in the chosen frequency interval for the $ICF_2C{=}O$ molecule is accidental, whereas their absence for $Fe(CO)_5$ and $Cr(CO)_6$ is natural.

The correlation under discussion becomes even more evident upon consideration of four-frequency resonances (see Figure 4). It can be seen that, as the density increases from 0.41 ($H(C{=}O)OC_2H_5$) to 8.17 cm ($C_4F_9C{=}OI$), the IVR time decreases from 20 to 2.4 ps. In this case, heavier ($C_4F_9C{=}OI$) and more compact ($ICF_2C{=}OF$, $(CF_3)_2C{=}C{=}O$, and $(CF_3)_2C{=}O$) molecules have, on the average, shorter IVR times compared to lighter and more extended ones ($H(C{=}O)OC_2H_5$ and $H_3C(C{=}O)OC_2H_5$). This fact is likely to mean that the so-called "local density" of resonances,[35] i.e., interactions of closely spatially arranged interatomic bonds, plays a determining role rather than the formally calculated total density of resonances.

$Fe(CO)_5$ and $Cr(CO)_6$ molecules also, at least, do not contradict the tendency that is observed for other compounds since very low densities of four-frequency resonances correspond to anomalously long IVR times. In addition, these densities appear mainly due to transitions in the ν_{CO} mode from "hot" bands. A sufficiently high density of resonances (>1 cm) in these molecules appears only for five-frequency resonances. However, interactions of higher orders are weaker; that is why the IVR from the ν_{CO} mode to remaining vibrational modes of the molecule proceeds so slowly.

C. Magnitude of the Intermode Interaction. Upon an increase in the vibrational energy in a given mode, the squared matrix element of the anharmonic interaction increases proportionally to the vibrational quantum number in the course of exchange of one quantum of this mode for quanta (two, three, etc.) of other vibrational modes. Therefore, the rate of the IVR should also increase. This conclusion is qualitatively confirmed by our experiments with the $ICF_2C{=}OF$ molecule, for which a decrease in the IVR time is observed with an increase in the level of the vibrational excitation of the molecule.

The kinetic dependences of the signal of the induced absorption Δk_{OD} that were obtained upon probing of successive vibrational transitions in the $ICF_2C{=}OF$ molecule are presented in Figure 5. To identify the position of each particular vibrational transition, we took a frequency shift of 20 cm^{-1}, which is close to the anharmonic shift of the C=O bond vibration (22 cm^{-1}), which we measured for this molecule from the frequency of the first overtone. It is seen that, with increasing vibrational energy level from that of the transition

dx.doi.org/10.1021/jp407131x | J. Phys. Chem. A XXXX, XXX, XXX−XXX

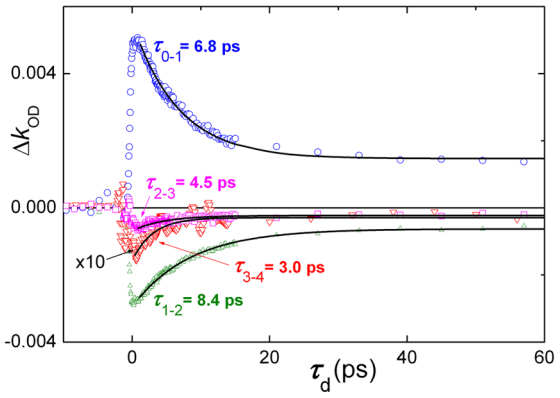

Figure 5. Dependences of the induced absorption signal Δk_{OD} on the delay time τ_d between the pump and probe pulses for successive vibrational transitions in $ICF_2C{=}OF$. Pressure of $ICF_2C{=}OF$, 30 Torr; laser fluence, 50 mJ/cm^2. Symbols correspond to experimental data, and solid curves are approximations of the decay by exponential functions. The values of Δk_{OD} for $\nu = 3 \rightarrow \nu = 4$ transition are multiplied by 10.

1−2 to that of the transition 3−4, the IVR time decreases from 8.4 to 3.0 ps. A comparatively small increase in the IVR time for the transition 1−2 compared to the transition 0−1 can be probably caused by mixing of a small share of a positive signal Δk_{OD} from the transition 0−1 with a negative signal from the transition 1−2. Previously,[26] upon probing of successive vibrational transitions in the $(CF_3)_2C{=}C{=}O$ molecule, we have not observed changes in τ_{IVR} upon an increase in the energy of the probed level. One of possible reasons for this could be a high error of determination of τ_{IVR} for high transitions.

D. Intermode Distribution. For the $ICF_2C{=}OF$ molecule, using the direct frequency scanning method, we also obtained the spectral dependence of Δk_{OD}, which is presented in Figure 6. Arrows in the figure show the positions of the maxima of the spectra of successive transitions for the C=O vibrational mode calculated for the value of their successive frequency shift of 20 cm^{-1} (see section C). This value provided the best fit of the spectral dependence of Δk_{OD}, which was

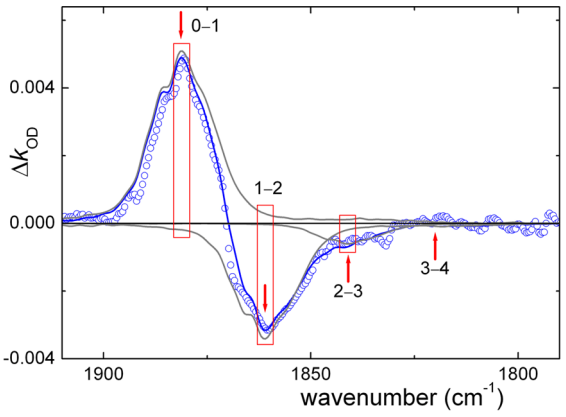

Figure 6. Spectral dependence of the induced absorption signal Δk_{OD} in the mode ν_1 = 1881 cm^{-1} of the $ICF_2C{=}OF$ molecule upon its multiphoton excitation. The radiation energy density is 50 mJ/cm^2, the pressure is 35 Torr, and the delay time is τ_d = 1.2 ps. Solid dark gray curves are the individual absorption bands and solid blue curve is the sum of these bands. Red bars indicate spectral intervals of signal integration (see text). Arrows indicate probed vibrational transitions.

obtained by the summation of the spectral bands from all the vibrational transitions beginning from $\nu = 0 \rightarrow \nu = 1$ to $\nu = 3 \rightarrow \nu = 4$. The sum of the areas of the experimental transient peaks differs from zero by about 10−15%. The area of the bleaching peak is a little bit bigger. It should be noted that the experimental transient spectra of Δk_{OD} measured for a number of other molecules have the similar tendency. This effect may be caused by different reasons: for instance, by systematic error of measurement or by the growing addition from the adjacent transitions due to a statistical inhomogeneous broadening of the bands of the excited vibrational states (see ref 27). The measurement accuracy of the direct scanning of the spectrum is rather low so the signal due to the transition $\nu = 3 \rightarrow \nu = 4$ is invisible on the background noise track. Nevertheless, this signal exists, and it was measured at a large signal accumulation (see appropriate curve in Figure 5). Red bars in Figure 6 demonstrate the spectral intervals of the signal integration. It is seen that, the admixtures of the signals from the adjacent transitions are rather negligible. The measured spectral dependence shows that the selective excitation of rather high levels of the ν_1 mode (up to $\nu = 3$ that corresponds to vibrational energy 5600 cm^{-1}) takes place since the magnitude of the signal due to the transition $\nu = 3 \rightarrow \nu = 4$ still remains measurable. However, it can be seen from the presented spectrum that, nevertheless, excited molecules reside mainly at the lowest levels $\nu = 1$ and $\nu = 2$, which is similar to the situation with the $(CF_3)_2C{=}C{=}O$ molecule that we observed previously.[26] By using experimental values of Δk_{OD} at the frequencies of corresponding transitions in the $ICF_2C{=}OF$ molecule, it is possible to estimate the average level of molecular excitation. For this purpose a system of rate equations for the relative population of levels under excitation may be solved similarly to work.[26] The calculations of the distribution of molecules over the levels of resonant ν_{CO} mode were made for Φ_{pump} = 50 mJ/cm^2 and for absorption cross-section of transition 0−1 $\sigma_{0,1} = 1.5 \times 10^{-18}$ cm^2 determined from the IR absorption peak. Under these conditions, 8.6% of molecules are excited from the initial states. It means that the average level of excitation of molecules is about 0.1 quanta per molecule.

E. Accumulating States Model. The IVR process in the $H_3C(C{=}O)OC_2H_5$ and $H_2C{=}CH(C{=}O)OC_2H_5$ molecules, which proceeds on two time scales with $\tau_1 \approx 6-8$ and $\tau_2 \approx 80$ ps (see Figure 2), should be considered independently. Initially, we pay attention to the following. After the excitation of the C=O chromophore group in a parent ethyl formate molecule $(H(C{=}O)OC_2H_5)$, a single-exponential decay of the state with a characteristic IVR time of 20 ps is observed. Upon replacement of the hydrogen atom in the H−C=O group by the methyl radical CH_3, a molecule of ethyl acetate, $CH_3(C{=}O)OC_2H_5$, is formed, for which the IVR process now proceeds in two stages, with their characteristic times being $\tau_1 = 6 \pm 1$ and $\tau_2 = 75 \pm 20$ ps. In this case, the contribution of the slow stage to the measured value of Δk_{OD} is relatively small, $B_1 \approx (2.8-3.3)B_2$ (see Table 1). Upon formation of an ethyl acrylate molecule, $H_2C{=}CH(C{=}O)OC_2H_5$, the hydrogen atom is replaced by a $H_2C{=}CH$ radical, and in this case, the characteristic times remain roughly the same, but the influence of the second stage of the IVR process becomes more pronounced, $B_1 \approx (0.7-0.9)B_2$.

To explain the occurrence of two stages, it seems natural to assume that the first, fast, stage of the process is related to a partial IVR to a group of states (conventionally, the first tier),

dx.doi.org/10.1021/jp407131x | J. Phys. Chem. A XXXX, XXX, XXX−XXX

which are likely to be located spatially closely to the bond under pumping. We will denote this group of states as $\mathcal{A}$. Then, two options are possible. In the first case, which is usually implied in works that explain the biexponentiality of the decay (see, e.g., ref 15), it is assumed that the second, slow, stage is caused by the IVR from $\mathcal{A}$ over the entire molecule (over $\mathcal{B}$ states; bath states), whereas the initial excited state (we denote it by $\mathcal{I}$) is coupled to $\mathcal{B}$ mainly via $\mathcal{A}$. The second option, which we consider to be more realistic for our two molecules, is that (see Figure 7) precisely $\mathcal{I}$ is directly coupled

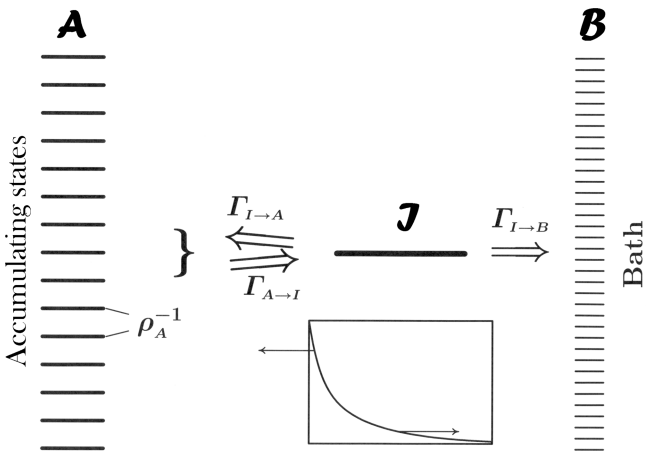

Figure 7. Illustration of the accumulating states model. The initial state $\mathcal{I}$ partially decays into a group of states $\mathcal{A}$, and then leakage from $\mathcal{A}$ through $\mathcal{I}$ into the bath states occurs on a longer time scale.

to $\mathcal{B}$; however, this coupling is weaker than that with $\mathcal{A}$, and as a consequence, at the second stage, the $\mathcal{I}$ state plays a role of a bottleneck for the IVR from $\mathcal{A}$ over the entire molecule.

Our reasoning is based on the following fact. The IVR time in a simpler parent $H(C{=}O)OC_2H_5$ molecule ($\tau_0 \approx 20$ ps) is substantially shorter than the time τ_2 in both molecules with the added radicals. Clearly, it is caused by the coupling $\mathcal{I} \Leftrightarrow \mathcal{B}$. It is unlikely that this coupling would be so weakened in new formations. However, a significant slowing down of the IVR process into $\mathcal{B}$ due to a fast redistribution of a considerable fraction of the initial excitation into $\mathcal{A}$ and, consequently, the formation of a bottleneck is quite realistic. A logical completion of the pattern is to assume that precisely the radical addition is responsible for the appearance of $\mathcal{A}$ states.

A simple phenomenological model that is based on kinetic equations for the populations N_I and N_A is considered in the Appendix. (The usage of the rate equations is justified with a good accuracy because in our experimental conditions we deal with very large ensembles of initial vibrational−rotational states (see, e.g., results of model calculations based on the Schrödinger equation and presented in refs 8 and 20).) In accordance with the notation of Figure 7, unknown rates of the forward and backward processes $\mathcal{I} \Leftrightarrow \mathcal{A}$ are introduced: $\Gamma_{I\to A}$ and $\Gamma_{A\to I}$. From experiment, values of characteristic times, which are related to eigenvalues A.3 of the system of eqs A.1 as: $\tau_1 = -\lambda_1^{-1}$ and $\tau_2 = \lambda_2^{-1}$, are taken. A variable parameter of the model is the rate $\Gamma_{I\to B}$ of the process $\mathcal{I} \Rightarrow \mathcal{B}$. In accordance with A.4, this parameter determines the two unknown rates and, in accordance with A.6 and A.7, it determines the contributions to the solution from the two exponentials: $C_{1,2}^{(I)}$ for the state $\mathcal{I}$ and $C_{1,2}^{(A)}$ for the group of states $\mathcal{A}$. In particular, for the state $\mathcal{I}$, we have

$$\frac{C_1^{(I)}}{C_2^{(I)}} = \frac{\Gamma_{I\to B}\tau_2 - 1}{1 - \Gamma_{I\to B}\tau_1} \tag{2}$$

Further, if we assume that the measured signal is determined only by the dynamics of the state $\mathcal{I}$; i.e., the ratio $C_1^{(I)}/C_2^{(I)}$ is equivalent to the ratio B_1/B_2 from Table 1, then we arrive at the following values for the variable parameter:

- $\Gamma_{I\to B}^{-1} \approx 23$ ps for the $H_3C(C{=}O)OC_2H_5$ molecule;
- $\Gamma_{I\to B}^{-1} \approx 48$ ps for the $H_2C{=}CH(C{=}O)OC_2H_5$ molecule.

Note that, for the first of these two molecules, the IVR time $\Gamma_{I\to B}^{-1}$ is very close to the IVR time in the parent $H(C{=}O)OC_2H_5$ molecule, which looks absolutely natural. At the same time, for the second molecule this time seems to be anomalously long.

Recall, however, that these estimates were obtained under the assumption that

$$\frac{B_1}{B_2} \equiv \frac{C_1^{(I)}}{C_2^{(I)}} \tag{3}$$

This assumption may well be incorrect. Indeed, the IVR in the group of states $\mathcal{A}$ can, in principle, *compensate the weaker bleaching* of the transition $0 \to 1$ in the ν_{CO} mode than the IVR to all the states $\mathcal{B}$. This effect of only partial compensation can be taken into account in terms of the following expression:

$$\frac{B_1}{B_2} = \frac{C_1^{(I)} + \beta C_1^{(A)}}{C_2^{(I)} + \beta C_2^{(A)}} \tag{4}$$

where the coefficient β is smaller than unity. From this, using eqs A.6 and A.7, we can determine to what extent the positive value of β affects the correctness of the determination of $\Gamma_{I\to B}$ and, conversely, what the value of β should be, if we assume that this rate is the same as that in the parent molecule.

Answers are given by the dependences presented in Figure 8 for both molecules. In particular, it is seen that, for $\Gamma_{I\to B}^{-1} = 20$ ps, the coefficient of compensation acquires the following values:

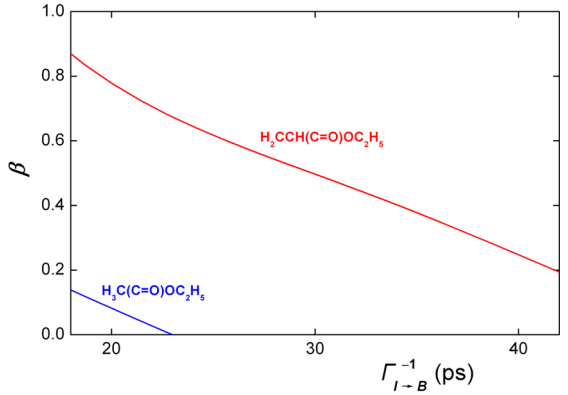

Figure 8. Relationship between the parameter β and the rate of IVR $\Gamma_{I\to B}$ from the initial state $\mathcal{I}$ to the bath states $\mathcal{B}$ complying the experimental values of τ_1, τ_2, and B_1/B_2 (see the text).

- $\beta = 0.08$ for the $H_3C(C{=}O)OC_2H_5$ molecule ($\Gamma_{I\to A}^{-1} = 11.7$ ps; $\Gamma_{A\to I}^{-1} = 22.5$ ps),
- $\beta = 0.77$ for the $H_2C{=}CH(C{=}O)OC_2H_5$ molecule ($\Gamma_{I\to A}^{-1} = 17.7$ ps; $\Gamma_{A\to I}^{-1} = 32$ ps),

dx.doi.org/10.1021/jp407131x | J. Phys. Chem. A XXXX, XXX, XXX−XXX

where, for completeness, the values of the rates of the forward and backward energy exchange between $\mathcal{I}$ and $\mathcal{A}$ are presented. Curves in Figure 8 determine compatible pairs of the values of the parameters $\Gamma_{I\to B}^{-1}$ and β that are set by experimentally determined characteristics of the biexponential decay.

F. Dilution Factor. As is known (see, e.g., refs 28 and 36), for large ensembles of states, a consistent quantum description of the competition between the process of decay of the state into a relatively dense spectrum and the reversal process leads to the notion of the dilution factor (denoted by the symbol σ), which is the relative average population of the initial state at $t \to \infty$. The knowledge of this quantity makes it possible to estimate the density of states of the molecule that are efficient with respect to the IVR process. In ref 20 (see also refs 8 and 19), a universal function has been calculated, which describes the dependence of σ on the product $x = \hbar W\rho$, where W is the initial rate of decay from the initial state to the ensemble of states with the density ρ that obey the statistics of the Gaussian orthogonal ensemble (GOE), which is typical for the dynamic chaos range.[37,38] From the viewpoint of the model that was considered in the preceding subsection, it is interesting to consider the question about the density ρ_A of states $\mathcal{A}$, which are efficient with respect to the first, fast, stage of the IVR process. In terms of eq A.1, the dilution factor that characterizes this stage is estimated as

$$\sigma \approx \frac{\Gamma_{A\to I}}{\Gamma_{I\to A} + \Gamma_{A\to I}} = \frac{1}{\Gamma_{I\to B}(\tau_1 + \tau_2 - \Gamma_{I\to B}\tau_1\tau_2)} \qquad (5)$$

where expression A.4 is used. Assuming, as was discussed above, that $\Gamma_{I\to B}^{-1} = 20$ ps, we obtain the following estimates:

- $\sigma \approx 0.34$ for the $H_3C(C{=}O)OC_2H_5$ molecule ($x \approx 0.9$; $\rho_A \approx 1.8$ cm),
- $\sigma \approx 0.36$ for the $H_2C{=}CH(C{=}O)OC_2H_5$ molecule ($x \approx 0.8$; $\rho_A \approx 3.0$ cm),

where, in the parentheses, the values of the parameter x that correspond to the function $\sigma(x)$ and of the quantity of interest ρ_A, which is found from the known value $W \equiv \Gamma_{A\to I}$, are given. Qualitatively, the obtained estimate is consistent with the fact that the density of states $\mathcal{A}$ involved at the fast stage of the IVR process should be greater for the larger attached radical. However, it should be noted that, in both cases, as our estimates show, the values of ρ_A are, at least, several times smaller than the total densities of states added to the molecule as a result of the attachment.

V. CONCLUSIONS

In this work, we investigated the intramolecular vibrational dynamics for nine molecules in their ground electronic state that was initiated by a mode-selective excitation of the C=O chromophore bond by resonant femtosecond IR laser radiation ($\lambda = 4.6$–5.8 μm). We used the method of IR pumping and IR probing of molecules in the gas phase with the spectral analysis of the probe radiation.

We examined three types of compounds, which differ in the number of C=O chromophores and in their arrangement. It turns out that the times of the IVR from the excited vibration and the character of this process are different for molecules of different types. Molecules with a single C=O bond to which a single atom can also be bonded ($(CF_3)_2C{=}C{=}O$, $(CF_3)_2C{=}O$, $C_4F_9C{=}OI$, $ICF_2C{=}OF$, and $H(C{=}O)OC_2H_5$) showed a simple monoexponential character of IVR with relatively short times, lying in the range 2.4–20 ps. In the $CH_3(C{=}O)OC_2H_5$ and $H_2CCH(C{=}O)OC_2H_5$ molecules, in which the C=O chromophore is inside of the molecule, the IVR proceeds on two time scales with strongly different characteristic times: $\tau_1 \approx 6$–8 and $\tau_2 \approx 80$ ps. The occurrence of two stages of IVR were interpreted in terms of the accumulating states model, which acceptably describes the experimental results we had so far. However, with additional experimental data, the model can be made more precise. In third-type molecules, $Fe(CO)_5$ and $Cr(CO)_6$, in which several C=O groups surround the central metal atom, the values of τ_{IVR} differ by two to three orders of magnitude from the IVR times of all the remaining molecules and lie in the nanosecond range, being ~1 and ~1.5 ns, respectively.

For the group of molecules with a single C=O chromophore, we observed that there is a correlation between the IVR time and the density of vibrational states in the vicinity of the first excited level. In this case, a shorter IVR time corresponds to a higher density of states. However, a more direct correlation is that between IVR times and the density of intermode anharmonic resonances, which proved to be the most clearly pronounced for four-frequency resonances. After the selective multiphoton excitation of the vibration of the C=O bond in the $ICF_2C{=}OF$ molecule, the probing of successive vibrational transitions showed a decrease in the IVR time with increasing level of the vibrational excitation of the molecule. These results agree with existing theoretical predictions.[4]

We also make a few remarks on the IR–IR pump–probe technique in combination with the spectral analysis of the probe radiation that we used in this work. As any other spectral technique, it has undeniable merits and certain restrictions, which should be taken into account upon its use. The basic restrictions are as follows. First, this method allows only to track the behavior of the spectrum of the molecule, i.e., of the change in the difference between the populations of vibrational levels, rather than of their absolute population. Nevertheless, under certain assumptions, it becomes possible to retrieve the distribution function of molecules over vibrational states, as this was done in our work.[26] Second, this technique works quite well if the bandwidth of the vibration under investigation is comparable or lower than its anharmonic shift. Otherwise, it is necessary to lower the temperature of the gas, e.g., with gas-dynamic cooling.

To a considerable extent, restrictions of this technique are compensated by its advantages. First, this technique is rather simple to be implemented experimentally. In addition, the most important merit of this technique is its rather high sensitivity. In the simplest variant, which we used in this work, the pump and probe radiation beams were reunited at a small angle to each other; therefore, the probe region was relatively small, 0.046 cm.[26] Nevertheless, this proved to be quite sufficient to measure Δk_{OD} signals from all the examined molecules. The passage to a collinear geometry makes it possible to increase the sensitivity of the method almost by an order of magnitude. A specific feature of our experiments was also that the broad spectrum of the femtosecond pump radiation (240 cm^{-1}) assuredly covered the absorption bands of the successive transitions within C=O vibration in the molecules under study. In combination with a fairly high energy density of the pump radiation, this ensured the excitation not only of the first level but also of several subsequent levels. In this case, comparable values of the absorption band widths of the molecules under investigation and of the anharmonic frequency

dx.doi.org/10.1021/jp407131x | J. Phys. Chem. A XXXX, XXX, XXX–XXX

shift of successive vibrational transitions (~20 cm^{-1}) made it possible to measure the times of the IVR from different vibrational levels of the molecule.

Summarizing all that was said above on the potential of the IR−IR pump−probe technique, we would like to cite the authors of ref 39 who, comparing the IR−IR pump−probe technique with the Raman probe method, said the following: "The present study shows that comparable information can also be obtained with IR pump−IR−probe spectroscopy avoiding the very weak Raman scattering process, provided that the molecule is small so that various hot bands are spectrally resolved, and provided that a reliable set of anharmonic constants is known from either theory or experiment." However, as our experiments showed, rather strict conditions that the authors of ref 39 imposed on the IR−IR pump−probe technique are, in fact, not so necessary, which makes it possible to obtain quite satisfactory results even for rather large and heavy molecules.

APPENDIX

The system of equations for the kinetic model shown in Figure 7 has the following form:

$$\frac{dN_I}{dt} = -(\Gamma_{I\to A} + \Gamma_{I\to B})N_I + \Gamma_{A\to I}N_A$$

$$\frac{dN_A}{dt} = \Gamma_{I\to A}N_I - \Gamma_{A\to I}N_A \quad (A.1)$$

The eigenvalues of the characteristic equation

$$(\lambda + \Gamma_{I\to A} + \Gamma_{I\to B})(\lambda + \Gamma_{A\to I}) - \Gamma_{I\to A}\Gamma_{A\to I} = 0 \quad (A.2)$$

which corresponds to this system, are

$$\lambda_{1,2} = -\frac{1}{2}(\Gamma_{I\to A} + \Gamma_{A\to I} + \Gamma_{I\to B}) \mp \frac{1}{2}\sqrt{(\Gamma_{I\to A} + \Gamma_{A\to I} + \Gamma_{I\to B})^2 - 4\Gamma_{A\to I}\Gamma_{I\to B}} \quad (A.3)$$

The variable parameter of the model is $\Gamma_{I\to B}$. Unknown rates are expressed via $\lambda_{1,2}$ and this parameter as follows:

$$\Gamma_{A\to I} = \frac{\lambda_1\lambda_2}{\Gamma_{I\to B}}, \quad \Gamma_{I\to A} = -(\lambda_1 + \lambda_2) - \Gamma_{I\to B} - \frac{\lambda_1\lambda_2}{\Gamma_{I\to B}} \quad (A.4)$$

Finally, the solution for the populations N_I and N_A with the initial conditions $N_I|_{t=0} = 1$, $N_A|_{t=0} = 0$ is given by

$$N_{I,A} = C_1^{(I,A)}\exp(\lambda_1 t) + C_2^{(I,A)}\exp(\lambda_2 t) \quad (A.5)$$

where

$$C_1^{(I)} = \frac{\lambda_1(\Gamma_{I\to B} + \lambda_2)}{\Gamma_{I\to B}(\lambda_1 - \lambda_2)}, \quad C_2^{(I)} = \frac{\lambda_2(\Gamma_{I\to B} + \lambda_1)}{\Gamma_{I\to B}(\lambda_2 - \lambda_1)} \quad (A.6)$$

$$C_1^{(A)} = -\frac{\lambda_1 + \lambda_2 + \Gamma_{I\to B} + \lambda_1\lambda_2/\Gamma_{I\to B}}{\lambda_1 - \lambda_2},$$

$$C_2^{(A)} = \frac{\lambda_1 + \lambda_2 + \Gamma_{I\to B} + \lambda_1\lambda_2/\Gamma_{I\to B}}{\lambda_1 - \lambda_2} \quad (A.7)$$

AUTHOR INFORMATION

Corresponding Authors

*(V.B.L.) Phone: +7 (495) 8510231. E-mail: laptev@isan.troitsk.ru.

*(E.A.R.) Phone: +7 (495) 8510578. E-mail: ryabov@isan.troitsk.ru.

Notes

The authors declare no competing financial interest.

ACKNOWLEDGMENTS

We are grateful to Dr. A. L. Malinovsky for useful discussions. This work was partially supported by the Russian Foundation for Basic Research, project nos. 08-02-00581 and 09-02-00495.

REFERENCES

(1) Bagratashvili, V. N.; Vainer, Y. G.; Dolzhikov, V. S.; Kol'yakov, S. F.; Makarov, A. A.; Malyavkin, L. P.; Ryabov, E. A.; Sil'kis, E. G.; Titov, V. D. Direct Observation by the RLS Method of the Randomization of the Vibrational Energy in Molecules During Interaction with a Strong Laser IR Field. *JETP Lett.* **1979**, *30*, 471−475.

(2) Zewail, A. H. Laser Selective Chemistry: Is it Possible? *Phys. Today* **1980**, *33*, 27−33.

(3) Hudgens, J. W.; McDonald, J. D. Energy Redistribution Observed in Infrared Multiphoton Excited C_2F_5Cl. *J. Chem. Phys.* **1981**, *74*, 1510−1511.

(4) Letokhov, V. S., Ed. *Laser Spectroscopy of Highly Vibrationally Excited Molecules*; Adam Hilger: Bristol, U.K., 1989.

(5) Uzer, T. Theories of Intramolecular Vibrational Energy Transfer. *Phys. Rep.* **1991**, *199*, 73−146.

(6) Lehmann, K. K.; Scoles, G.; Pate, B. H. Intramolecular Dynamics from Eigenstate-Resolved Infrared Spectra. *Annu. Rev. Phys. Chem.* **1994**, *45*, 241−274.

(7) Nesbitt, D. J.; Field, R. W. Vibrational Energy Flow in Highly Excited Molecules: Role of Intramolecular Vibrational Redistribution. *J. Phys. Chem.* **1996**, *100*, 12735−12756.

(8) Makarov, A. A.; Malinovsky, A. L.; Ryabov, E. A. Intramolecular Vibrational Redistribution: from High-Resolution Spectra to Real-Time Dynamics. *Phys.-Usp.* **2012**, *55*, 977−1007.

(9) Windhorn, L.; Witte, T.; Yeston, J. S.; Proch, D.; Motzkus, M.; Kompa, K. L.; Fuss, W. Molecular Dissociation by Mid IR Femtosecond Laser Pulses. *Chem. Phys. Lett.* **2002**, *357*, 85−90.

(10) Windhorn, L.; Yeston, J. S.; Witte, T.; Fuss, W.; Motzkus, M.; Proch, D.; Kompa, K. L.; Moore, C. B. Getting Ahead of IVR: A Demonstration of Mid-Infrared Molecular Dissociation on Sub-Statistical Timescale. *J. Chem. Phys.* **2003**, *119*, 641−645.

(11) Apatin, V. M.; Kompanets, V. O.; Laptev, V. B.; Matveets, Y. A.; Ryabov, E. A.; Chekalin, S. V.; Letokhov, V. S. Excitation and Dissociation of Polyatomic Molecules under the Action of Femtosecond Infrared Laser Pulses. *Russ. J. Phys. Chem. B* **2007**, *1*, 113−119.

(12) Witte, T.; Yeston, J. S.; Motzkus, M.; Heilweil, E. J.; Kompa, K. L. Femtosecond Infrared Coherent Excitation of Liquid Phase Vibrational Population Distributions ($v > 5$). *Chem. Phys. Lett.* **2004**, *392*, 156−161.

(13) Heilweil, E. J.; Casassa, M. P.; Cavanagh, R. R.; Stephenson, J. C. Population Lifetimes of OH($v = 1$) and OD($v = 1$) Stretching Vibrations of Alcohols and Silanols in Dilute Solution. *J. Chem. Phys.* **1986**, *85*, 5004−5018.

(14) Banno, M.; Sato, S.; Iwata, K.; Hamaguchi, H. Solvent-Dependent Intra- and Intermolecular Vibrational Energy Transfer of $W(CO)_6$ Probed with Sub-Picosecond Time-Resolved Infrared Spectroscopy. *Chem. Phys. Lett.* **2005**, *412*, 464−469.

(15) Yoo, H. S.; DeWitt, M. J.; Pate, B. H. Vibrational Dynamics of Terminal Acetylenes: I. Comparison of the Intramolecular Vibrational Energy Redistribution Rate of Gases and the Total Relaxation Rate of Dilute Solutions at Room Temperature. *J. Phys. Chem. A* **2004**, *108*, 1348−1364.

(16) Yoo, H. S.; DeWitt, M. J.; Pate, B. H. Vibrational Dynamics of Terminal Acetylenes: II. Pathway for Vibrational Relaxation in Gas and Solution. *J. Phys. Chem. A* **2004**, *108*, 1365−1379.

(17) Yoo, H. S.; DeWitt, M. J.; Pate, B. H. Vibrational Dynamics of Terminal Acetylenes: III. Comparison of the Acetylenic C−H Stretch

Intramolecular Vibrational-Energy Redistribution Rates in Ultracold Molecular Beams, Room-Temperature Gases, and Room-Temperature Dilute Solutions. *J. Phys. Chem. A* **2004**, *108*, 1380−1387.
(18) Malinovsky, A. L.; Makarov, A. A.; Ryabov, E. A. Real-Time Observation of the Dynamics of Vibrational-Energy Redistribution within an Isolated Polyatomic Molecule by Spontaneous Raman Spectroscopy. *JETP Lett.* **2004**, *80*, 532−534.
(19) Malinovsky, A. L.; Doljikov, Y. S.; Makarov, A. A.; Ogurok, N.-D. D.; Ryabov, E. A. Dynamics of Intramolecular Vibrational Redistribution in Propargylchloride Molecule Studied by Time-Resolved Raman Spectroscopy. *Chem. Phys. Lett.* **2006**, *419*, 511−516.
(20) Malinovsky, A. L.; Makarov, A. A.; Ryabov, E. A. Intramolecular Vibrational Dynamics of Propyne and Its Derivatives: The Role of Vibrational−Rotational Mixing. *JETP* **2008**, *106*, 34−45.
(21) Makarov, A. A.; Malinovsky, A. L.; Ryabov, E. A. A Novel Feature of Intramolecular Vibrational Redistribution in Propargyl Alcohol and Propargyl Amine. *J. Chem. Phys.* **2008**, *129*, 116102.
(22) Malinovsky, A. L.; Makarov, A. A.; Ryabov, E. A. Extremely Slow Intramolecular Vibrational Redistribution: Direct Observation by Time-Resolved Raman Spectroscopy in Trifluoropropyne. *JETP Lett.* **2011**, *93*, 124−128.
(23) Makarov, A. A.; Malinovsky, A. L.; Ryabov, E. A. Slow Intramolecular Vibrational Redistribution: the Latest Results for Trifluoropropyne, a Comparison with the Other Terminal Acetylenes and the Mechanism. *Phys. Scr.* **2012**, *85*, 058102.
(24) Stromberg, C.; Myers, D. J.; Fayer, M. D. Vibrational Dynamics of Large Hot Molecules in the Collisionless Gas Phase. *J. Chem. Phys.* **2002**, *116*, 3540−3553.
(25) Kompanets, V. O.; Laptev, V. B.; Makarov, A. A.; Pigulsky, S. V.; Ryabov, E. A.; Chekalin, S. V. Direct Observation of the Vibrational Energy Redistribution in $(CF_3)_2CCO$ Molecules Resonantly Excited by Femtosecond Infrared Laser Radiation. *JETP Lett.* **2010**, *92*, 135−139.
(26) Chekalin, S. V.; Kompanets, V. O.; Laptev, V. B.; Pigul'sky, S. V.; Makarov, A. A.; Ryabov, E. A. Intramolecular Vibrational Dynamics in Bis (Trifluoromethyl)Keten Excited by Resonant Femtosecond IR Radiation. *Chem. Phys. Lett.* **2011**, *512*, 178−183.
(27) Makarov, A. A.; Petrova, I. Y.; Ryabov, E. A.; Letokhov, V. S. Statistical Inhomogeneous Broadening of Infrared and Raman Transitions in Highly Vibrationally Excited XY_6 Molecules. *J. Phys. Chem. A* **1998**, *102*, 1438−1449.
(28) Stewart, G. M.; McDonald, J. D. Intramolecular Vibrational Relaxation from C−H Stretch Fundamentals. *J. Chem. Phys.* **1983**, *78*, 3907−3915.
(29) Kim, H. L.; Kulp, T. J.; McDonald, J. D. Infrared Fluorescence Study on the Threshold of Intramolecular Vibrational State Mixing. *J. Chem. Phys.* **1987**, *87*, 4376−4382.
(30) Bagratashvili, V. N.; Kuzmin, M. V.; Letokhov, V. S.; Stuchebrukhov, A. A. Theory of Multiple-Photon IR Excitation of Polyatomic Molecules in the Model of Active and Passive Modes of a Vibrational Reservoir. *Chem. Phys.* **1985**, *97*, 13−29.
(31) Stuchebrukhov, A. A.; Marcus, R. A. Theoretical Study of Intramolecular Vibrational Relaxation of Acetylenic CH Vibration for v = 1 and 2 in Large Polyatomic Molecules $(CX_3)_3YCCH$, where X = H or D and Y = C or Si. *J. Chem. Phys.* **1993**, *98*, 6044−6061.
(32) Marshall, K. T.; Hutchinson, J. S. Excited-State Preparation and Relaxation in the Vibrational Quasicontinuum. *J. Chem. Phys.* **1991**, *95*, 3232−3243.
(33) Zhang, Y.-F.; Marcus, R. A. Intramolecular Dynamics II. Artificial Intelligence Search Evaluation Function and Treatment of Resonance Centers for Large Systems. *J. Chem. Phys.* **1992**, *96*, 6065−6072.
(34) Kerstel, E. R. T.; Lehmann, K. K.; Mentel, T. F.; Pate, B. H.; Stoles, G. Dependence of Intramolecular Vibrational Relaxation on Central Atom Substitution: ν_1 and $2\nu_1$ Molecular Beam Optothermal Spectra of $(CH_3)_3CC{\equiv}CH$ and $(CH_3)_3SiC{\equiv}CH$. *J. Phys. Chem.* **1991**, *95*, 8282−8293.
(35) Bigwood, R.; Gruebele, M.; Leitner, D. M.; Wolynes, P. G. The Vibrational Energy Flow Transition in Organic Molecules: Theory Meets Experiment. *Proc. Natl. Acad. Sci. U.S.A.* **1998**, *95*, 5960−5964.
(36) Bixon, M.; Jortner, J. Intramolecular Radiationless Transitions. *J. Chem. Phys.* **1968**, *48*, 715−726.
(37) Wigner, E. P. Random Matrices in Physics. *SIAM Rev.* **1967**, *9*, 1−23.
(38) Ott, E. *Chaos in Dynamical Systems*; Cambridge University Press: New York, 1993.
(39) Botan, V.; Hamm, P. J. Intramolecular Vibrational Energy Relaxation in Nitrous Acid (HONO). *Chem. Phys.* **2008**, *129*, 164506.